Chemical Engineering Journal 116 (2006) 85–95

Chemical Engineering Journal

www.elsevier.com/locate/cej

Individual impeller flooding in aerated vessel stirred by multiple-Rushton impellers

Andrej Bombač *, Iztok Žun

Laboratory for Fluid Dynamics and Thermodynamics, Faculty of Mechanical Engineering, University of Ljubljana, Aškerčeva 6, 1000 Ljubljana, Slovenia

Received 26 April 2005; received in revised form 18 October 2005; accepted 19 October 2005

Abstract

The paper presents flooding detection in the dispersion of air into water in a stirred vessel equipped with a multiple-turbine impeller. All experiments were performed in a pilot-size mixing vessel using single, dual and triple Rushton turbine impellers. Deionized water and compressed air were used as a working fluid. The flooding recognition method based on resistivity probe response was applied, defining impeller flooding as the appearance of ragged cavities behind the blades of the individual impellers. Classifying the flooding regimes into a simple generalized flow map gave the sequence of impeller flooding: spreading from the lowest impeller flooding subsequently to the upper impellers. A comparison of our individual impeller-flooding data with the results found in the literature is shown for single impeller and partially for dual- and triple-turbine impeller, where due to the lack of published data only a comparison for the lowest turbine was possible.

Keywords: Stirred vessel; Multiple impeller; Aerating; Impeller flooding

1. Introduction

Nowadays vessels with a high liquid aspect ratio are usually used in fermentation processes. Such fermenters are basically equipped with multiple impellers to improve hydrodynamic characteristics and consequently mass and heat transfer. In broth fermentation the rheological properties change from the beginning to end of the process. A change from a Newtonian to a pseudo-plastic fluid causes a change in viscosity of up to four orders of magnitude, which strongly affects the bulk flow field in a vessel. The question arises of how this transformation exerts an influence on flooding. This phenomenon is dependent on the input rates of gas flow and power dissipated into the broth via two-phase impeller flow discharge. A low gas input flow rate causes insufficient dissolved oxygen in the liquid bulk, while an excessively high gas flow rate may lead to the appearance of dead zones and flooding. If it still occurs, in some special occasions it does not have any influence on, e.g. micromixing effects in an aerated tank [15] nor does the aeration always affect the mixing number in the same way; it can either decrease or increase it [11]. In the work of Alves and Vasconcelos [2] it is shown that even in a flooding regime their mixing model and correlation of mixing time can be used for multiple impeller stirring. The findings of Sardeing et al. [30] studying the aeration in the vicinity of the liquid surface with a specially composed multistage impeller showed a compromise choice between a high gas flooding rate (partial flooding) and a long bubble plume length in a vessel.

Among the first researchers studying the flooding phenomenon, Mikulcova et al. [20] and Rushton and Bimbinet [29] described the term ‘flooding’. Since then several authors have researched this phenomenon. In the literature, the term flooding has often been used to describe a transition to unsatisfactory operation of a stirrer in a tank, while the definition of flooding is still not well established. In addition, many different experimental methods have been reported for the measurements of hydrodynamic regimes once flooding appears. As derived from single impeller studies, these methods can be divided into two groups: (i) techniques based on global measurements (such as gas holdup, power drawn) combined with visual observation of two-phase flow circulation through the vessel wall and (ii) techniques based on local two-phase characteristics such as fluid velocity and local void fraction of the impeller discharge flow, measured with a constant temperature anemometer, resistivity probe, micro-propeller or vibrating vane. Furthermore, the

* Corresponding author. Tel.: +386 1 4771 406; fax: +386 1 4771 447.
E-mail address: andrej.bombac@fs.uni-lj.si (A. Bombač).

1385-8947/$ – see front matter © 2005 Elsevier B.V. All rights reserved.
doi:10.1016/j.cej.2005.10.009

Nomenclature

b	impeller blade length (m)
c	impeller clearance above the base (m)
d	impeller disk diameter (m)
D	stirrer diameter (m)
f	baffle width (m)
f_b	impeller blade frequency (s^{-1})
Fl	Flow number, $q/(nD^3)$
Fr	Froude number, Dn^2/g
Fr_T	tank Froude number, Tn^2/g
g	gravity (m/s^2)
h	distance between the impellers (m)
H	liquid height (m)
i_b	number of impeller blades
k_1, k_2	correlation coefficients
M	torque (Nm)
Mo	Morton number, $g\eta^4/(\sigma^3)$
n	impeller frequency (s^{-1})
n_b	impeller blade frequency (s^{-1})
P	ungassed power (W)
q	volumetric gas flow rate (m^3/s)
R	regression coefficient
s	sparger clearance above the base (m)
T	tank diameter (m)
w	impeller blade width (m)
We	Weber number, $\rho n^2 D^3/\sigma$
z	number of turbines

List of symbols

α	local void fraction (%)
η	viscosity (Pa s)
ρ	liquid density (m^3/kg)
σ	surface tension (N/m)

manner of achieving flooding should be described more precisely according to the flow regime transition. Changing of the flow regime from loading to flooding (LFT) or flooding to loading (FLT) corresponds to regimes which constitute hysteresis. Another question arises if the hysteresis is of negligible effect, as found by Warmoeskerken and Smith [33] or not, e.g. [1,14,17,20,22,27]. Such significant confusion found in the literature regarding the term flooding can be best seen in the flow regime map, see Fig. 1, which takes into consideration data for a vessel of diameter 0.45 m and D/T equal to 0.33. It can be seen that the FLT of devices at pilot or industrial scale at Fr = const is achieved at markedly higher Fl values than those at laboratory scale regardless of whether the prediction includes the D/T ratio or not.

1.1. Single-turbine impeller

Using global measurements of gas holdup and power drawn in air liquid mixing, flooding was defined as a state (varying the impeller speed at constant gas flow rate) when there was

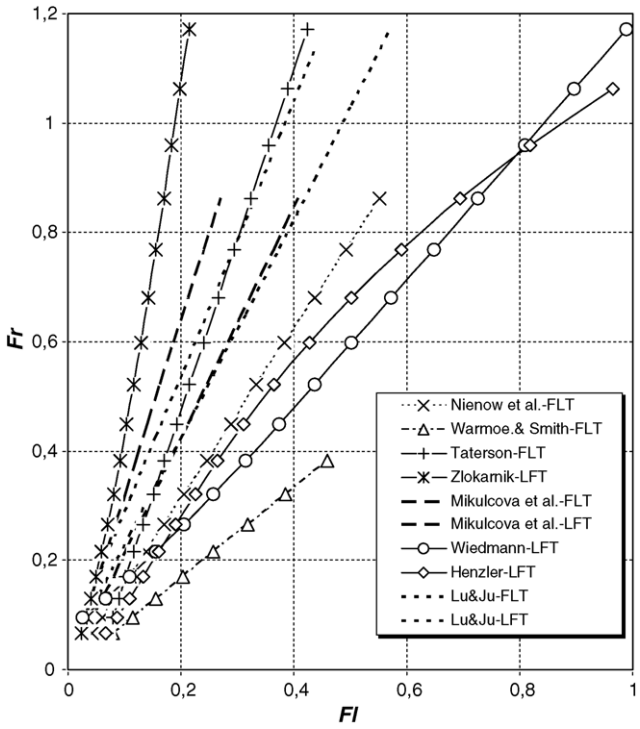

Fig. 1. Comparison of literature data regarding the term 'flooding'.

no more horizontal flow of gas starting from the impeller and reaching the wall [29]. The flooding point was defined with a sharp decrease of the holdup for a given total power, which corresponds with visual observations of the flow patterns on the vessel wall. Mikulcova et al. [20] postulated the criterion for impeller flooding considering the hysteresis range, i.e. LFT and FLT in the dispersing of air into water with a single disk turbine. The method was based on the minimal impeller speed technique combined with conductivity measurements of the liquid near the impeller. Wiedmann [35] and Nienow et al. [21] detected the onset of flooding from changes of the gassed power drawn; the flooding point was defined by step change in the gassed power curve under constant impeller speed and varying gas rate. According to Warmoeskerken and Smith [34] the flooding transition reflects the unique states of the two-phase flow around the stirrer. Based on the qualitative determination of the liquid radial outflow vector near the stirrer with a micropropeller, a new definition of impeller flooding was introduced. In this regime there is an axial flush of gas through the impeller plane up to the free liquid surface with no radial discharge two-phase flow. Lu and Chen [16] studied the flooding phenomenon by using a conical hot-film anemometer. The onset of flooding was postulated with sharp transition of r.m.s. turbulent fluctuation velocity of the impeller-discharge liquid flow. Later Lu and Ju [17] examined the gas-filled cavity formation, flooding transition and pumping capacity of an aerated disk turbine. The flooding was determined on the basis of the impeller-discharge fluid velocity change. According to Hudcova et al. [13,14] the effect of liquid height and impeller clearance on the FLT were studied based on changes of the gassed power curves. Only the change of liquid height itself had no effect on FLT, while

increasing the impeller clearance had a similar effect to the gas dispersion process with a ring sparger of diameter greater than the impeller. Tatterson and Morrison [32], based on a retrofitting of Zweitering's experimental data, analyzed the effect of tank to impeller diameter ratio on LFT. Their model is an extension of the previous work of Warmoeskerken and Smith [33] and Biesecker (as cited by Tatterson and Morrison [32]). Paglianti et al. [24] presented a simple method based on non-intrusive detection of conductance fluctuations for the detection of FLT in a stirred tank. A later work [25] provided a mechanistic model for predicting the LFT in an aerated vessel stirred by Rushton turbine. The model neglects the influence of sparger size, as well as impeller clearance and liquid height.

1.2. Multiple-turbine impellers

A survey of the literature shows that only few studies have been published concerning flooding in multiple-turbine driven tanks. Henzler [12] presented the criterion based on dimensionless numbers of the LFT for single impeller stirring and for the lower impeller in multiple impeller stirring. The criterion was extrapolated from the measured data of other researchers on standard Rushton turbine stirring. In a study [31] the impeller gas-filled cavity structures were presented for a triple impeller. Detection of cavities was performed with a vibrating vane mounted on the vessel wall; findings were obtained on the basis of frequency analysis of pressure pulses of the vane. Structures were classified into a flow regime map where a clear delineation between loading and flooding regimes was given for the lowest impeller while for the middle and uppermost impellers it was only indicated. Nocentini et al. [23] reported qualitative observations of two-phase flow field in a vessel with a four-stage impeller. Only at a very low impeller speeds and at high gas flow rates were all the turbines flooded; with an increase of impeller speed the turbines became loaded sequentially. A sharp transition of power drawn was found for the lowest impeller whereas the transition was gradual and rather undefined for the other turbines. In their study of air–water dispersion with dual impellers, Hudcova et al. [14] used a special shaft with two strain gauges, enabling individual impeller torque measurements. On this basis the flooding was detected for each impeller separately and was defined either from the step change in the gassed power curve or visually. LFT appeared differently for each impeller and was strongly dependent on their clearance (Δh). Compared to a single impeller the lower impeller required a higher speed to achieve a FLT (by $\Delta h/D \leq 1.5$) otherwise when the full independent flow patterns are present the lower FLT can be estimated reasonably well by the equation of Nienow et al. [21]. Abrardi et al. [1] examined dissipated power and mixing time in a sparged vessel driven with a dual turbine for different hydrodynamic regimes including the flooding of the lower impeller. The findings of Alves and Vasconcelos [2] are interesting, presenting some new aspects of mixing in gas–liquid contactors with triple impeller stirring. Some properties, e.g. mixing time, can be still evaluated even in the flooding regime; otherwise more data on flooding could not be obtained even in recent reviews: e.g. [10,18,26].

The purpose of this paper is to enable the simple estimation of individual impeller flooding for single-, dual- and triple-turbine impellers in the dispersion of air into water. The experimental method using resistivity probe response has been described in detail in [6–8]. The method enabled the recognition of the following cavity structures: vortex-clinging structure VC, the appearance of the first large cavity 1L, two large cavities 2L, small ′3-3′ structure S33, large ′3-3′ structure L33 and ragged cavities RC, respectively. The RC structure corresponded to the flooding regime while the loading regime could form the L33 or S33 structure.

In multiple-turbine stirring the lower turbine became flooded first, followed by the middle impeller and finally the upper impeller successively by increasing the gas flow rate. The LFT of the lower turbine in the dual- and triple-turbine systems occurred at noticeably lower gas flow rates than that in single-turbine stirring, while the upper impeller became flooded at higher gas flow rates. Good agreement with flooding prediction data from the literature was found for single-turbine stirring and for the lowest impeller in dual- and triple-turbine stirring. Otherwise a comparison of our results with those from the literature was not possible for the middle and upper impellers due to a lack of data in the literature.

2. Experimental

A cylindrical flat-bottomed Perspex vessel of 450 mm ID with four baffles mounted perpendicularly to the vessel wall was used. The geometrical details for the stirred vessel can be found in Fig. 2. Deionized water and compressed air at room temperature were used as working fluids in all experiments. In multiple-turbine stirring the liquid height in the vessel was increased by the distance between turbines. Impeller speed was measured by IR-pulse transmitter with an absolute error of ± 1 rpm. An HBM transducer enabled torque measurements with error of ± 0.02 Nm, while the gas flow rate was measured with calibrated rotameters with the following errors: $\pm 0.4\ m^3/h$ for measuring tubes from 5 to 25 m^3/h, and $\pm 0.14\ m^3/h$ for measuring tubes from 1 to 8 m^3/h, respectively. At the highest flow rates two rotameters were connected in parallel. The experimental setup is depicted in Fig. 3 with the indicated optical window located on the vessel wall at the lower impeller height to enable visualization of the impeller discharge flow. A high-speed monochromatic video camera, a Weinberger VISARIO with a Nikon 50/2 focus lens and a CMOS image sensor and optimized noise reduction was used in the case of dispersing with single impeller. A high recording rate was needed at 4000 images/s at electronic shutter speed 200 μs. The image size format at such a speed was set to 768 × 512 pixels, with a pixel size of 10 μm. Recording time span was up to 4 s which produced up to 12 Gb of data in a single experimental run

In order to obtain local information on gas filled cavity structures, a microresistivity probe of 11 μm tip size was used, located in the close vicinity of the outer edge of the impeller blade. At the lowest impeller speed at least 600 cavities were detected for further statistical treatment. Measurements were always performed in the same manner starting from low to high impeller

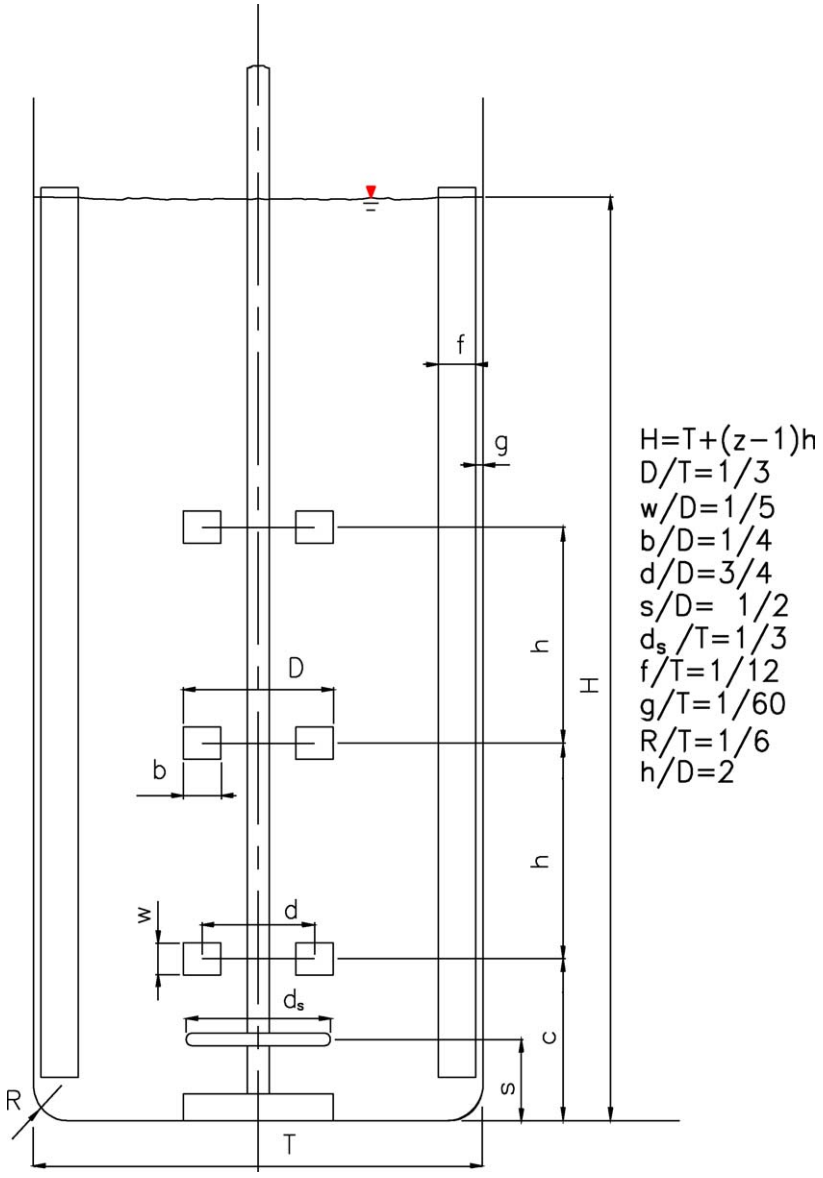

Fig. 2. Geometrical parameters of the vessel and stirrers.

speeds, with stepwise increasing of the gas flow rate at constant impeller speed. The reproducibility and directional sensibility was assumed to be equal to those evaluated in [6].

The LFT can be detected by rapid reduction of void fraction in a turbine discharge two-phase flow, as well by gas-filled cavity structures change. Some experimental studies of gas-filled cavity structures and local void fraction distribution in water–air dispersion have been presented [6,7,8,16,17]. While Lu an Ju [17] studied gas-filled cavity configuration, flooding and pumping capacity using a constant temperature anemometer in single-turbine stirring, in [7,8,37] gas-filled cavity structures and local void fraction based on resistivity probe response in an aerated vessel stirred with single and dual Rushton disk impellers were investigated. Furthermore, in [5], attention was paid to gas-filled cavity structures in aerating in a pseudo-plastic fluid such as a CMC-water dilution. Full details of the experimental work outlined here and the criterion for gas-filled cavity structure recognition have been described in detail in [6]. Local detection of the phases was performed by the resistivity probe producing voltage response as a corresponding structural function [38]:

$$M_{\mathrm{p}}(x,t) = \begin{cases} 1, & x \text{ is occupied by } p \\ 0, & x \text{ is occupied by } p \end{cases} \quad p = \{\mathrm{L}, \mathrm{G}, \mathrm{S}\} \tag{1}$$

In a two-phase flow field at a particular point x three phase states p are possible at any time t: the liquid phase L, gas phase G or phase interface S, respectively. Using a discrete fourier transformation of the structural function M_{p} enabled the presentation of the significant frequencies of an appearing gas phase. The fourier coefficients X_{k} were obtained from:

$$X_{\mathrm{k}} = \Delta t \sum_{k=0}^{N-1} M_{\mathrm{p}}(t_{\mathrm{k}})\, \mathrm{e}^{-\frac{j2\pi ik}{N}} \tag{2}$$

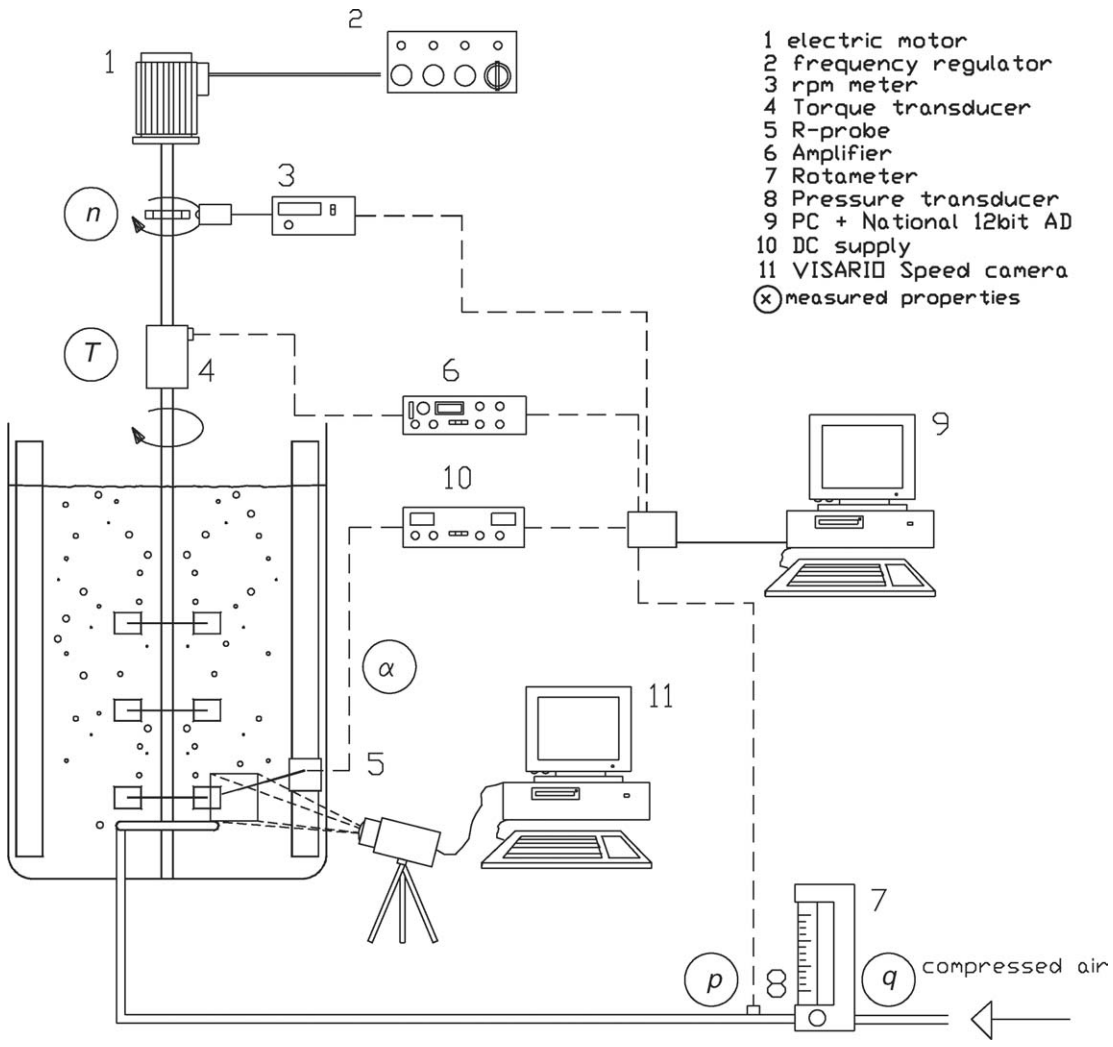

Fig. 3. Experimental setup.

where Δt denotes the time interval between successive instants t_i. Among fourier coefficients X_k that correspond to the frequency $k/(N\Delta t)$ only coefficients from $k=0$ to $(N/2)-1$ are meaningful. From the given criterion the following gas-filled cavity structures were recognized: vortex-clinging structure (VC), structure with one large cavity (1L), structure with two large cavities (2L), small ′3-3′ structure (S33), large ′3-3′ structure (L33) and ragged cavity structure (RC). In Fig. 4 the resistivity probe responses and their fast fourier transformations are shown for the above mentioned structures. The development of the cavity structures follows from the top to bottom, i.e. from the VC to RC structure, respectively. From the probe response over longer periods of observation it was evident that large cavities were present on the same blades. The beginning of the S33 structure in the frequency-domain can be seen from the appearance of a significant fourier coefficient at frequency $f_b/2$, which increases in accordance with increasing of the gas flow rate. This pattern was taken as a criterion of S33 structure recognition. The L33 structure is a combination of three smaller and three larger large cavities that is a combination of large cavities exclusively. The alternating sequence of smaller and larger large cavities was also quite evident in the L33 structure. From the evolution of fourier coefficients in the frequency domain (with increasing gas flow rate) the increase of the coefficient at $f_b/2$ is obvious. At the point when both coefficients $f_b/2$ and f_b are nearly equal, the L33 structure was recognized, as depicted in Fig. 4.

The method used here was recently compared with two other experimental methods, i.e. the global gas holdup method and power drawn method in a standard mixing vessel equipped with a single Rushton turbine [9] where the results were in good agreement among themselves. Given the fact that air-dispersing was performed with a single Rushton impeller, all the changes at the local level (impeller) are reflected at the global one (gas holdup, power drawn) which actually enables the application of the global methods.

3. Results and discussion

3.1. Single-turbine impeller

Ragged cavities are in good agreement with the findings in [21,31,33,34] where the delimitation between “loading” and

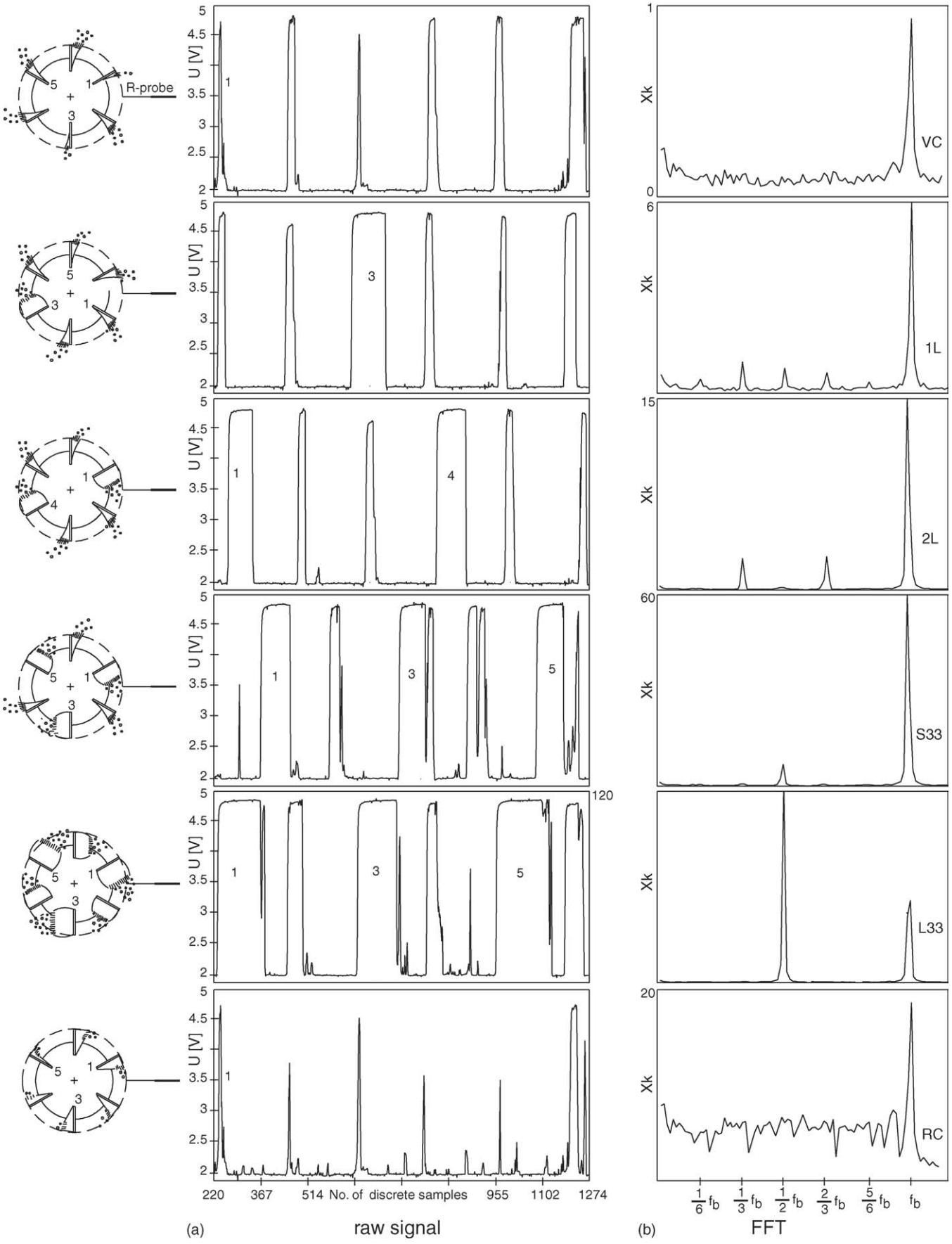

Fig. 4. Cavity structures and corresponding probe response (a) and frequency transformation (b).

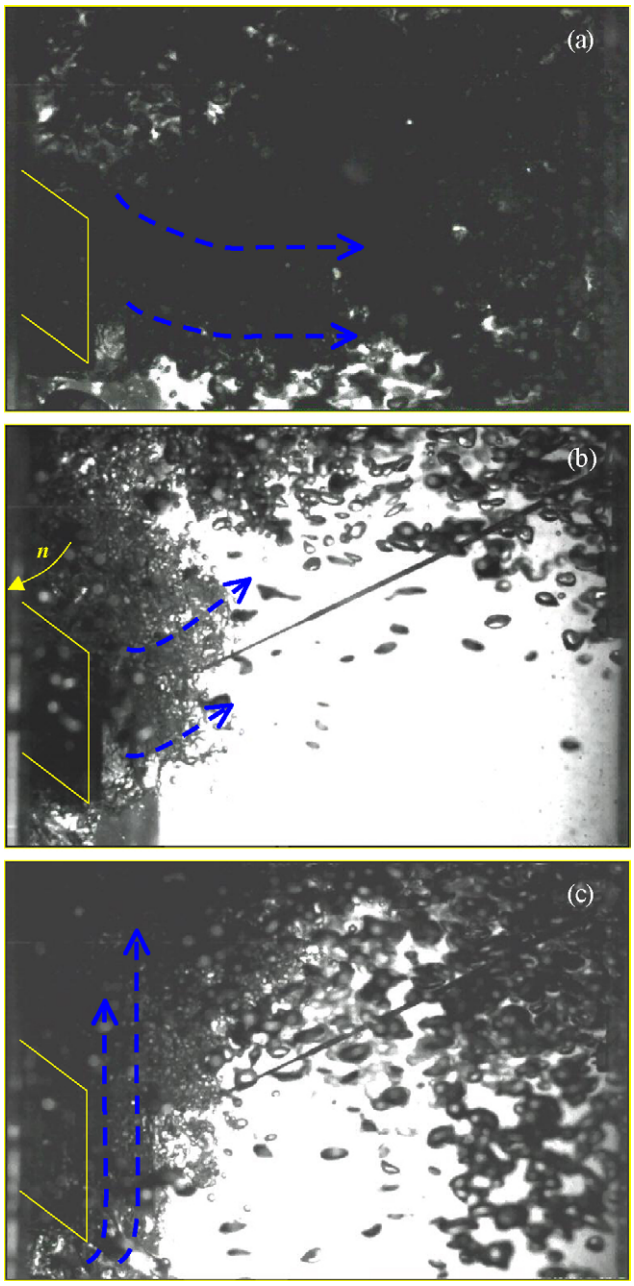

Fig. 5. Photos of discharge two-phase flow in (a and b) loading and (c) flooding regime, respectively.

"flooding" corresponding to ′3-3′ or large clinging cavity structure and RC was shown. Using a high speed camera in our experimental work some distinctiveness in the form of discharge two-phase flows can be seen from the side view as shown in Fig. 5. Photos of the discharge two-phase flow were taken at constant impeller frequency 4.45 s^{-1} and three different gas flow rates; 6 m^3/h (a), 7 m^3/h (b) and 8 m^3/h (c), respectively. In case (a) a radially oriented discharge flow was observed with typical L33 structures. Despite being under the same L33 structure, increasing of the gas flow rate led to the change of the discharge flow direction, i.e. from radial to upward, respectively, as depicted in case (b). This state was found as the last possible loading regime, while a further increment of gas caused impeller flooding, case (c). Here clouds of bubbles moved from the gas sparger past the impeller upward to the free surface. Flooding was recognized with the presence of the RC structure. Such a hydrodynamic regime was marked (with the increasing of the gas flow rate at constant impeller speed) with an adequate set of (n_F and q_F) as "impeller flooding" and the transition to flooding as LFT, respectively. The corresponding correlation of the experimental data was preferred in the same type as in [2,3,19,21] to predict impeller flooding in single- and multiple- turbine impellers:

$$Fl_F = k_1 \cdot Fr_F^{k_2} \tag{3}$$

where k_1, k_2 and regression coefficient R are given in Table 2. The experimental results are depicted in Fig. 6 as separate marks. At lower impeller speeds corresponding to $Fr < 0.08$ the LFT occurred at the appearance of RC structure deriving from VC structure while at higher impeller speeds RC structure derived from ′3-3′ structure, which is in good agreement with previous results [6].

To enable a comparison between experimental results and the data from the literature, only correlations of LFT transition are taken and depicted in Fig. 6. The geometrical configurations with respect to D/T ratio, impeller spacing, sparger, etc. of the experimental setups are shown in Table 1.

Regarding the vessel scale, as can be seen in Fig. 6, the following conclusions can be drawn: the predicted LFT appeared in larger vessels than ours [12,35] at somewhat higher Fl values, and in smaller vessels the predicted LFT appeared at lower Fl values [17,20]. The experiment in [1] in which LFT appeared at lower Fl values was also carried out in a smaller vessel than ours.

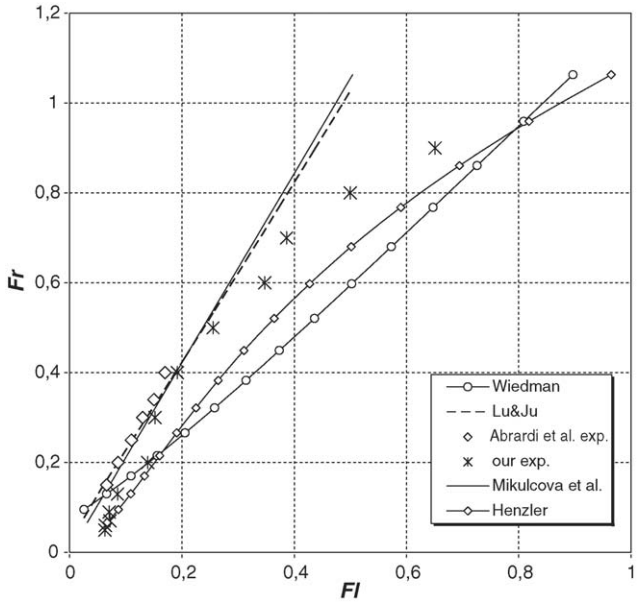

Fig. 6. Comparison of our experimental LFT results in single-turbine stirring with those from the literature.

Table 1
Summary of the geometrical conditions in impeller flooding detection

Author	Prediction	Flow regime	T (m)	D/T	c/T	h/T	Sparger	Detection
Mikulcova et al. [20]	$Fl_F = \frac{100}{6.11 \pm 1.24} Fr \left(\frac{T}{D}\right)^{-3.43}$	$Fr \leq 0.9$	0.19, 0.31	0.2 –0.39	1/3	–	Tube	LFT, FLT
Zlokarnik [36]	$Fl_F = 0.19 Fr_F^{0.75}$	$0.1 \leq Fr \leq 2$	0.2, 0.45	0.2 –0.45	1/3	–	Tube	LFT
Henzler [12]	$Fl_F = \frac{0.21 Fr_F^{2.1(D/T)}}{(T/D-2.04)^{1.3}} + \frac{0.14 Fr_F^{7.54(D/T)}}{(T/D-2.25)^{1.5}}$, $(\Delta h/T) > 0.75$	$Re > 1 \times 10^4$, $Fr \leq 5$	Ind. scale	0.3 –0.4	–	–	Ring, tube	LFT
Wiedman [35]	$Fl_F = 0.973 \left(-0.15 + \sqrt[4]{Mo} + 0.05 \ln \frac{We}{Fr}\right) Fr^a + 0.2 Fr^{1.6}$, where $a = 0.605 + \left(\ln \frac{We}{Fr}\right)^{-1}$	$0.1 \leq Fr \leq 1.5$	0.45 –1.5	1/3	1/6	–	Ring	LFT
Nienow et al. [21]	$Fl_F = 30(D/T)^{3.5} Fr_F$	$Fr_F \leq 0.85$	0.29 –1.2	0.33 –0.5	0.25,0.4	–	Ring	FLT
Wamoeskerken and Smith [34]	$Fl_F = 1.2 Fr_F$	$Fl \leq 0.36$	0.44 –1.2	0.4	0.4	–	Ring	FLT
Hudcova et al. [14]	Exper. data	$Fl \leq 0.16$	0.56	1/3	1/3	0–1	Ring	FLT
Smith et al. [31]	Exper. data	$Fr \leq 1$, $Fl \leq 1$	0.64	0.4	–	0.08–1	Two rings	LFT FLT
Tatterson and Mor-rison [32]	$(Fl_F - 0.6 Fr_F) = -0.031 Fr_{T,F}(T/D) + 0.046$, $2 \leq Fr_{T,F}(T/D) \leq 64$, retrofitted literature data							
Lu and Ju [17]	$n_F = A(T/D)^{1.167}(gq/D^4)^{0.333}(4.07 + 1.21 i_b - 0.147 i_b^2)$ $A =$ 0.064(FLT) or 0.072(LFT)	$Fr \leq 1.3$, 0.28	0.25 –0.5	1/3	–	–	Ring	LFT, FLT
Nocentini et al. [22]	Exper. data	$Fr \leq 0.2$	0.23, 0.39, 0.57	0.2 –0.5	1/3–3/5	–	Ring	LFT, FLT
Nocentini et al. [23]	Exper. data	$Fr \leq 0.2$	0.23	0.52	0.5	1	Ring	LFT, FLT
Abrardi et al. [1]	Exper. data	$Fr \leq 2.5$, $Fl \leq 0.2$	0.39, 0.65	1/3	1/3	2/3	8 × 2 mm h	LFT, FLT
Alves and Vasconcelos [2]	$Fl_F = 0.33 Fr_F^{0.69}$	$Fl < 0.25$	0.292	1/3	1/2	1	Ring	LFT
Paglianti et al. [24]	Comp. code	$Fr \leq 0.3$, $Fl \leq 0.15$	0.2, 0.72	0.33	1/3	–	Ring, p.plate	FLT

3.1.1. Multiple-turbine impeller

Defining the hydrodynamic regimes in multiple-turbine stirring is more complex. Treating of the bulk liquid flow with one circulation loop per impeller is admissible only with $h/D = 1.5$ as proposed in [4,13,31], otherwise the impellers generate a common interactive discharge flow. The LFT of the lower and upper turbines occurred similarly as in single-turbine stirring via different cavity structure development. In dual-turbine stirring, the transition corresponded to the appearance of the RC structure developed from VC, 1L, 2L at $Fr < 0.08$, and from ′3-3′ structures at higher Fr, respectively. But quite a big difference between the lower and upper turbine arises with respect to the gas dispersing ability. As can be seen in Fig. 7, the upper turbine remained in a loading regime at markedly higher Fl values (when it became flooded) than the lower one. This is in good agreement with our previous findings in [8]. Otherwise in dual-turbine stirring with impeller spacing $h/D = 1.5$ a common interactive flow was produced where the flooding transition of the lower turbine occurs at higher gas flow rates than that of single-impeller stirring.

As the impellers separate, fully independent flow patterns occur, and from the literature survey it seems that such cases were mainly studied and oriented toward the flooding of the lower turbine only. In such manner as proposed in [12], the LFT of the lower turbine can be estimated reasonably well by using the same prediction as for single impeller stirring. The conclusions of Hudcova et al. [14] and Smith et al. [31] were similar, both used the prediction of Nienow et al. [21] for single impeller stirring. Thus the given estimations can be explained comparing the individual impeller flooding conditions of multiple-turbine and single-turbine stirring as depicted in Fig. 7. The LFT of the lower turbine (Du1) occurred at much lower gas flow rates than in single-turbine stirring. As can be seen from visual observation through the vessel wall, two-phase circulation in the liquid bulk ceased due to reduced liquid pumping capacity of the lower turbine, so the liquid bulk in the close vicinity and especially below

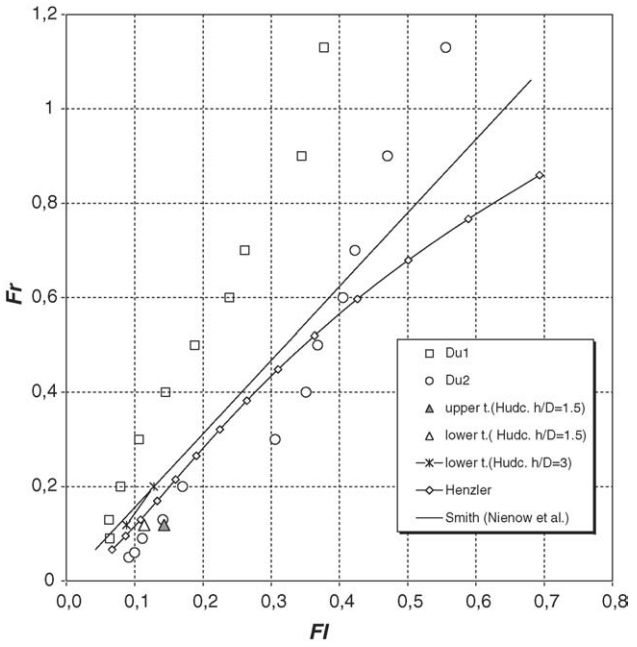

Fig. 7. Experimental results: individual impeller flooding in dual-turbine stirring compared with those from the literature.

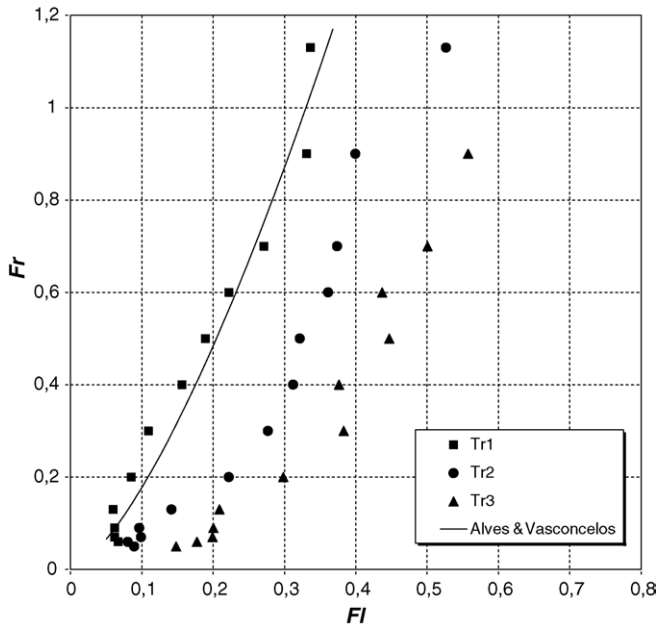

Fig. 8. Experimental results: individual impeller flooding in triple-turbine stirring compared with those from the literature.

the lower turbine remained undispersed. Below the lower turbine and between the turbines no circulation was seen. Passing the lower turbine, the sparged air rose close around the impeller shaft toward the upper turbine and entered it. Major two-phase circulation appeared in the horizontal plane of the turbine and above it. With further increasing of the gas flow rate the upper turbine (Du2) also became flooded. As depicted in Fig. 7, the upper turbine achieved flooding transition at somewhat higher gas flow rates compared to single turbine stirring. On that basis, taking the single-impeller criterion as a guide for the prediction of lower impeller flooding in dual-turbine stirring seemed to be a satisfactory estimation for practical use, which is also indicated in [3,19].

When three equal turbines are mounted on the same shaft, spaced by at least 1.5D, the lowest impeller will become flooded long before the upper ones have ceased to function properly. Based on visual observation it was clearly seen that the turbines became flooded in correspondence with the increasing of the gas flow rate. When the lower one was flooded the two-phase circulation in the liquid bulk was very similar to that in dual turbine stirring. Major two-phase circulation was found in the horizontal planes of the middle and upper turbine. Further increasing of the gas flow rate led to the flooding of the middle turbine. When these two turbines were flooded no circulation was seen below the middle turbine and the liquid bulk remained undispersed. In this situation the sparged air entered the upper turbine actually undispersed. Discharging two-phase flow was still able to preserve its own circulation. Finally, with the increasing of gas flow rates the upper turbine became flooded. In Fig. 8 the LFT for the lower (Tr1), middle (Tr2) and upper turbine (Tr3) is shown. At the lower turbine LFT occurred changing from VC, 1L, 2L to RC at $Fr < 0.09$ and from ′3-3′ to RC structure at higher Fr, while the middle and upper impeller became flooded changing from VC to RC at $Fr < 0.2$ and from ′3-3′ to RC structure at higher Fr, respectively. For a comparison of our results with data from the literature, only the work of Alves and Vasconcelos [2] studying the mixing in gas–liquid contactors agitated by triple Ruston turbines in the flooding regime was available. Comparing both results it was found that their suggested correlation actually represented the LFT for the lower turbine as can be seen in Fig. 8. Their results are in very good agreement with ours. Such a basis can support the evaluation of why modelling of mixing and dimensionless correlation of mixing time can be possible even in a flooding regime (the lowest impeller) – since the middle and upper impellers are still operating under a loading regime. In [23] a qualitative observation of a two-phase flow field in a lab scale vessel with a four-stage turbine impeller is presented. Only at very low impeller speeds and high gas flow rates were all the turbines flooded; with the increasing of the impeller speed the turbines became correspondingly loaded, which is in good agreement with our findings.

All experimental data of individual impeller LFT were correlated using Eq. (3) with adequate parameters shown in Table 2 the corresponding curves are depicted in Fig. 9. In general, major differences concerning gas dispersing ability can be found between the lower, middle and upper turbines. Comparing the results of individual impeller LFTs of triple-, dual- and single-

Table 2
Corresponding coefficients to Eq. (3)

Impeller configuration	k_1	k_2	R
Single turbine (Single)	0.5007	0.7710	0.974
Dual: upper turbine (Du2)	0.5387	0.6133	0.989
Dual: lower turbine (Du1)	0.3337	0.7962	0.980
Triple: upper turbine (Tr3)	0.5829	0.4371	0.989
Triple: middle turbine (Tr2)	0.4901	0.6003	0.986
Triple: lower turbine (Tr1)	0.2990	0.6437	0.965

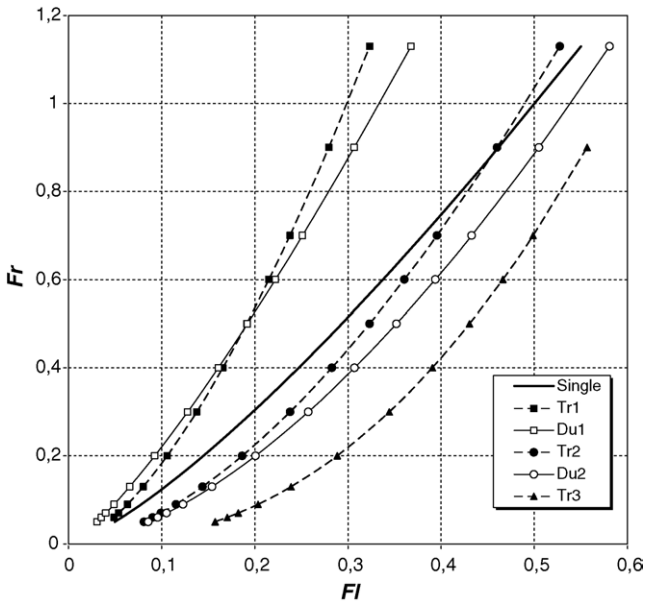

Fig. 9. Individual impeller flooding conditions; comparison of single, dual and triple-impeller stirring.

turbine stirring, the following conclusions can be drawn: the upper turbine of the triple turbines achieved the highest *Fl* values when it became flooded. From this point of view a triple impeller as a unit is capable of dispersing the largest amount of air, followed by dual impeller and single impeller, respectively. Furthermore, the LFT of the lower turbine in dual turbines coincides with the LFT of the lower turbine in triple turbines, as well as the coincidence of the LFT of the middle turbine in triple turbines with the LFT of the upper turbine in dual turbines. Our experimental data are consistent with the flooding relationship suggested in [28] as well as with the expectations in [31] by which the LFT of the upper impellers would occur at a *Fl* number about twice that which floods the lowest.

To avoid dead zones at the bottom part of the vessel it is important to know the flooding timing. By increasing the gas flow rate, the bottom impeller became flooded first, followed by the middle one and finally the upper. Therefore, the lowest turbine was found to be the most critical for ensuring good overall performance of a reactor which becomes flooded at remarkably lower *Fl* values compared to that of single turbine stirring. Knowing the flooding point of the upper impellers could be useful in some special occasions when the lower impeller is already flooded, such as micromixing effects in an aerated tank [15], the effect of aeration on the mixing number [11], use of mixing time correlation in multiple impeller stirring [2] or the use of a specially composed multistage impeller working at a high gas flooding rate [30].

At this point it should be emphasized that all experiments were carried out in an air/water system. The presented results could therefore serve only as an orientation for the practical analysis of fermenters at the beginning of the process when the fermentation broth behaves in an aqueous manner. Moreover, the pilot-size vessel had a fixed *D*/*T* ratio which can not be taken a priori when subjected to scaled up design. However, the authors believe that the data could be valuable as a benchmark test for CFD analysis that could be applicable to industrial size vessels.

4. Conclusions

The paper presents the individual impeller flooding conditions in air dispersing into water stirred with a multiple-turbine impeller. Based on local detection of the gas phase in a turbine-discharge two-phase flow and appropriate procedure, it was shown that the loading to flooding transition occurred via the development of different gas filled cavity-structures irrespective of single- or multiple-turbine stirring. This is the first time that individual impeller flooding conditions with dual- and triple-turbine impellers in a pilot-size aerated stirred vessel have been detected and classified in a flow regime map.

The experimental results of flooding recognition in single-turbine stirring were in good agreement with comparable ones found in the literature. Comparing our experimental data with data from the literature it can be seen that the loading to flooding transition appears at somewhat higher *Fl* values in stirring in larger vessels than ours and at lower *Fl* values in smaller ones.

Flooding transition of the lower turbine in dual-turbine stirring occurred at lower gas flow rates than that of single-turbine stirring, while the upper impeller remained in a loading regime in spite of marked increasing until it become flooded.

In triple-impeller stirring the turbines became flooded in correspondence with the increasing of the gas flow rate. The lower impeller became flooded first, followed by the flooding of the middle turbine and finally the upper turbine, respectively. Considering the composite impeller as a unit, the triple turbine impeller was capable of dispersing the largest amount of air and the single impeller the smallest amount.

Experimental data on the loading to flooding transition of the lower turbine with dual turbines coincide with those of the lower turbine in triple turbines, as well as the data of the upper turbine in dual-turbine stirring with those of the middle turbine in triple-turbine stirring. These findings can be explained by stable independent flow circulations of each individual impeller. Our results were consistent in all cases with those for which experimental data or correlations can be found in the literature.

Acknowledgments

This work was financially supported by the Slovenian Ministry of Higher Education, Science and Technology under contract No. P2-162.

References

[1] V. Abrardi, G. Rovero, G. Baldi, S. Sicardi, R. Conti, Hydrodynamics of a gas-liquid reactor stirred with a multiple-impeller system, Trans. Inst. Chem. Eng. A 68 (1990) 516.
[2] S.S. Alves, J.M.T. Vasconcelos, Mixing in the gas–liquid contactors agitated by multiple turbines in the flooding regime, Chem. Eng. Sci. 50 (14) (1995) 2355.
[3] A. Bakker, J.M. Smith, K.J. Myers, How to disperse gases in liquids, Reprint from Chemical Engineering, December 1994, by McGraw-Hill Inc.

[4] A. Bombač, Effects of geometrical parameters on Newton number in an aerated stirred tank, J. Mech. Eng. 44 (3–4) (1998) 105.
[5] A. Bombač, I. Žun, M. Žumer, J. Turk, Zbornik Kuhljevi dnevi 1996, Slovensko društvo za mehaniko, Ljubljana, 1996, pp. 193–198 (in Slovene).
[6] A. Bombač, I. Žun, B. Filipič, M. Žumer, Gas-filled cavity structures and local void fraction distribution in aerated stirred vessel, AIChE J. 43 (11) (1997) 2921.
[7] A. Bombač, I. Žun, Gas-filled cavity structures and local void fraction distribution in vessel with dual impellers, Chem. Eng. Sci. 55 (2000) 2995.
[8] A. Bombač, I. Žun, A simple method for detecting individual impeller flooding of dual Rushton impellers, in: Proceedings of the European Conference on Mixing X, Elsevier Science B.V., 2000, pp. 469–476.
[9] A. Bombač, I. Žun, Flooding recognition methods in a turbine stirred vessel, J. Mech. Eng. 48 (12) (2002) 663.
[10] P.R. Gogate, A.A.C.M. Beenackers, A.B. Pandit, Multiple-impeller systems with a special emphasis on bioreactors: a critical review, Biochem. Eng. J. 6 (2) (2000) 109.
[11] F. Guillard, C. Trägårdh, Mixing in industrial Rushton turbine-agitated reactors under aerated conditions, Chem. Eng. Process 42 (5) (2003) 373.
[12] H.J. Henzler, Verfarentechnishe Auslegungsunterlagen fur Ruhrbehalter als Fermenter, Chem. Ing. Tech. 52 (5) (1982) 461.
[13] V. Hudcova, A.W. Nienow, W. Haozhung, L. Huoxing, On the effect of liquid height on the flooding/loading transition, Chem. Eng. Sci. 42 (2) (1987) 375.
[14] V. Hudcova, V. Machon, A.W. Nienow, Gas-liquid dispersion with dual Rushton turbine impellers, Biotechnol. Bioeng. 34 (1989) 617.
[15] W.W. Lin, D.J. Lee, Micromixing effects in aerated stirred tank, Chem. Eng. Sci. 52 (21–22) (1997) 3837.
[16] W. Lu, H. Chen, Flooding and critical impeller speed for gas dispersion in aerated turbine-agitated vessels, Chem. Eng. J. 33 (1986) 57.
[17] Wei-Ming Lu, Shin-Jon Ju, Cavity configuration, flooding and pumping capacity of disc-type turbines in aerated stirred vessel, Chem. Eng. Sci. 44 (2) (1989) 333.
[18] R. Mezaki, M. Mochizuki, K. Ogawa, Engineering Data on Mixing, Elsevier, Amsterdam, 2000.
[19] N. Harnby, M.F. Edwards, A.W. Nienow, Mixing in the Process Industries, 2nd ed., Butterworths Heinemann, Oxford, 1992.
[20] E. Mikulcova, V. Kudrna, J. Vlcek, Bestimmung der Grenzbedinungen fuer die Ueberflutung des Ruehrers K1, Scientific paper of the Institute of Chemical Technology, Prague, 1967, p. 167.
[21] A.W. Nienow, M.M.C.G. Warmoeskerken, J.M. Smith, M. Konno, On the flooding/loading transition and the complete dispersal condition in aerated vessels agitated by a Rushton-turbine, in: Proceedings of the 5th European Conference on Mixing, BHRA, The Fluid Engineering Centre Cranfield, Bedford, UK, 1985, pp. 143–154.
[22] M. Nocentini, F. Magelli, G. Pasquali, Some comments on the flooding-loading transition for gas–liquid vessels stirred with Rushton turbines, Chem. Eng. Res. Des. 66 (1988) 378.
[23] M. Nocentini, F. Magelli, G. Pasquali, D. Fajner, A fluid dynamic study of a gas–liduid, non-standard vessel stirred by multiple impeller, Chem. Eng. J. 37 (1988) 53.
[24] A. Paglianti, S. Pintus, M. Giona, Time-series analysis approach for the identification of flooding/loading transition in gas–liquid stirred tank reactors, Chem. Eng. Sci. 55 (2000) 5793.
[25] A. Paglianti, Simple model to evaluate loading/flooding transition in aerated vessels stirred by Rushton disc turbines, Can. J. Chem. Eng. 80 (2002) 660.
[26] E.J. Paul, V.A. Atiemo-Obeng, S.M. Kresta, Handbook of Industrial Mixing, John Wiley and Sons, Hoboken, NJ, 2004.
[27] M. Roustan, M.Z.A. Bruxelmane, CHISA, Prague, (1981), paper B3.3.
[28] M. Roustan, Power consumed by the Rushton turbines in non standard vessel under gassed conditions, in: Proceedings of the 5th European Conference on Mixing, BHRA, The Fluid Engineering Centre Cranfield, Bedford, UK, 1985, pp. 127–141.
[29] J.H. Rushton, J.J. Bimbinet, Hold-up and flooding in air–water mixing, Can. J. Chem. Eng. 46 (1968) 16.
[30] R. Sardeing, F. Ferrand, M. Poux, P. Avrillier, C. Xuereb, Hydrodynamics and gas dispersion characterization in a system equipped with a new gas-inducing impeller, Chem. Eng. Technol. 26 (1) (2003) 31.
[31] J.M. Smith, M.M.C.G. Warmoeskerken, E. Zeef, Flow conditions in vessel dispersing gases in liquids with multiple impellers, in: C.S. Ho, J.Y. Oldshue (Eds.), Biotechnology Processes, AIChE, 1987, p. 107.
[32] G.B. Tatterson, G.L. Morison, Effect to tank to impeller diameter ratio on flooding transition for disk turbines, AIChE J. 33 (10) (1987) 1751.
[33] M.M.C.G. Warmoeskerken, J.M. Smith, The flooding transition with gassed Rushton turbines, Fluid Mixing II, Symposium Series No. 89, 1985, 59.
[34] M.M.C.G. Warmoeskerken, J.M. Smith, Flooding of disk turbines in gas–liquid dispersions: a new description of the phenomenon, Chem. Eng. Sci. 40 (11) (1985) 2063.
[35] J.A. Wiedmann, Zum Ueberflutunverhalten Zwei- und Dreiphasig Betriebener Rhuerreaktoren, Chem. Ing. Tech. 55 (9) (1983) 689.
[36] M. Zlokarnik, Ruhrleistung in begasten flussigkeiten, Chem. Ing. Tech. 45 (10a) (1973) 689.
[37] I. Žun, A. Bombač, An application of local void fraction measurements in discharge flow of single and dual Rushton impellers, in: Proceedings of the Mixing IX – Multiphase Systems, GFGP, Paris-Marne La Vallee, 1997, pp. 153–160.
[38] I. Žun, B. Filipič, M. Perpar, A. Bombač, Phase discrimination and void fraction measurements via genetic algorithms, Rev. Sci. Instrum. 66 (10) (1995) 5055.